Macromolecules

COMMUNICATION TO THE EDITOR

pubs.acs.org/Macromolecules

Polymer Dynamics of Polybutadiene in Nanoscopic Confinement As Revealed by Field Cycling ^{1}H NMR

M. Hofmann,[†] A. Herrmann,[†] S. Ok,[‡] C. Franz,[§] D. Kruk,[†,∥] K. Saalwächter,[§] M. Steinhart,[‡] and E. A. Rössler*[,†]

[†]Experimentalphysik II, Universität Bayreuth, D-95440 Bayreuth, Germany

[‡]Institut für Chemie, Universität Osnabrück, Barbarastr. 7, D-46069 Osnabrück, Germany

[§]Institut für Physik-NMR, Martin-Luther-Universität Halle-Wittenberg, Betty-Heimann-Str. 7, D 06120 Halle, Germany

INTRODUCTION

Applying electronic (fast) field cycling (FC) NMR, Kimmich and co-workers have performed extensive studies on the collective dynamics in (bulk) polymer melts.[1] As a result, a generic dispersion behavior has been found for the dipolar fluctuations of polymer segments. The NMR relaxation dispersion exhibits characteristic power-law regimes and shows a crossover from a dispersion predicted by the Rouse model for short polymer chains to that of entangled polymer dynamics which can be described by the renormalized Rouse formalism. According to these works, the relaxation power laws observed for entangled polymers do not follow those expected from the tube-reptation model, introduced first by de Gennes[2] and further developed by Doi and Edwards.[3] This is a challenging statement because currently the well-established reptation model offers the most successful concept of polymer dynamics.

Kimmich, Fatkullin, and co-workers[4−6] have also reported FC NMR results on polymers confined in nanoporous solid-state matrices supporting the idea that the tube-reptation model is indeed applicable for polymers in confinement. Independently of the polymer chain length, i.e., below as well as above M_e (the entanglement molecular weight), the NMR relaxation dispersion shows the characteristic power-law behavior of the tube-reptation model. More precisely, the regime II of the tube-reptation model has been identified. Surprisingly, confinement effects have been observed for confinement sizes in the range of 5−1000 nm, i.e., for sizes in most cases much larger than the size of a single polymer chain. The phenomenon has been called "corset effect" and explained as a finite size phenomenon which leads to reptation in a tight effective tube of diameter corresponding to the nearest-neighbor distance (which is much smaller than the typical size of the effective tube of the tube-reptation model in the bulk melt). Recently, the results have been questioned by neutron scattering (NS) experiments.[7,8] Studying polymers in 40 nm confinement, the authors have reported a slowing down of the dynamics in the Rouse regime whereas no change has been observed for the glassy ("local") dynamics, and a strong corset effect has been ruled out. In response, Kimmich and Fatkullin pointed out the important difference in observing potential confinement effects in terms of dynamic structure factor (NS) vs orientation autocorrelation functions (NMR),[9,10] claiming a higher sensitivity to confinement effects of the latter. Applying static ^{1}H double-quantum (DQ) NMR probing reorientation correlations at long times, Ok et al.[11] have found a relatively weak confinement effect when investigating the dynamics for polybutadiene (PB) in self-ordered anodic aluminum oxide matrices (AAO). A 2−3 nm layer in proximity to the neutral confining wall has been identified, within which the isotropization of chain motion due to reptation appears to be suppressed, or at least much protracted.

In a recent series of papers of the Bayreuth group, polymer dynamics in the bulk have been reinvestigated by means of FC ^{1}H NMR.[12−15] Frequency−temperature superposition (FTS), commonly employed in rheology of polymers,[16] has been applied in order to extend the accessible frequency window of FC NMR. Therewith we have been able to monitor the dynamics of PB over more than 6 decades in amplitude and 8 decades in frequency, encompassing segmental as well as collective polymer dynamics. These results have been combined with the data from ^{1}H DQ NMR of Vaca Chávez and Saalwächter,[17] which almost perfectly extend the FC ^{1}H NMR data up to even lower frequencies (longer times) into the reptation (III) and free-diffusion regimes (IV) of the tube-reptation model. This large set of data suggests the possibility of an interpretation alternative to that given by Kimmich and Fatkullin.[1] The NMR relaxation behavior of bulk entangled polymers, which appears to follow the predictions of the renormalized Rouse formalism,[1] can be attributed to a highly protracted transition from Rouse dynamics to fully established tube reptation. The latter has been observed at $Z = M/M_e > 100$, and the necessary frequency (or time) window is at the moment only accessible by ^{1}H DQ NMR. Only for such high molecular weights some qualitative predictions of the tube-reptation model have been confirmed, though a deviation from the theoretical power-law exponent still prevails even at the highest M.[17] Actually, this has been the first time that regime III and even regime IV have been reached experimentally. In accordance with rheological[19,20] as well as dielectric experiments,[21] we claim that the crossover to full tube-reptation dynamics occurs only above another characteristic molecular weight $M_r \gg M_e$.

In the light of this reinterpretation of the FC NMR relaxation features in bulk polymers, the interpretation of the FC NMR results reported for polymers in confinement by Kimmich, Fatkullin, and co-workers becomes ambiguous. The present contribution addresses this problem directly, using the same method but for another well-defined model nanocomposite as in ref 11.

Received: February 3, 2011
Revised: May 3, 2011
Published: May 16, 2011

The corset effect has been observed for polymers such as poly(ethylene oxide) and perfluoropolyether in different confinements of various sizes up to ca. 1000 nm.[4−6] In the present contribution, we report on FC ^{1}H NMR results for PB embedded in AAO membranes, which, just as the previously investigated systems,[11] are expected to provide a simple geometric hard-wall confinement with only weak polymer−surface interactions. Results for bulk PB and PB infiltrated in AAO membranes with pore diameters of 60 and 20 nm are discussed. The samples are prepared in the same way as those in the paper of Ok et al.[11] Since FC NMR is able to probe polymer dynamics on a very short time scale which is not accessible by DQ NMR, the present work is meant to complement the previous DQ ^{1}H NMR results and to validate the corset effect.

EXPERIMENTAL SECTION

A STELAR FFC 2000 relaxometer was applied that allows measuring the dispersion of the ^{1}H spin−lattice relaxation time T_1 in the frequency window of 10 kHz−20 MHz. The shortest measurable T_1 lies around 1 ms. Our final results are shown in the susceptibility representation.[12] According to the fluctuation−dissipation theorem, the susceptibility $\chi''(\omega)$ can be expressed by the spectral density $J(\omega)$ as $\chi''(\omega) = \omega J(\omega)$. Thus, the Bloembergen, Purcell, Pound expression for the spin−lattice relaxation rate assumed to hold for polymer melts with isotropic dynamics[1,22]

$$1/T_1(\omega) = C[J(\omega) + 4J(2\omega)] \quad (1)$$

can be converted to[12]

$$\omega/T_1(\omega) = C[\chi''(\omega) + 2\chi''(2\omega)] \equiv 3C\chi''_{\mathrm{NMR}}(\omega) \quad (2)$$

The factor 3 is introduced to keep the integral over $\chi''_{\mathrm{NMR}}(\omega)$ normalized to $\pi/2$. In the case of negligible intermolecular relaxation contributions, the spectral density $J(\omega)$ is given as Fourier transform of the orientational correlation function of rank two. Assuming FTS, the NMR susceptibility spectra collected at 11 or more temperatures in the range of 210−400 K are merged to yield a master curve $\chi''_{\mathrm{NMR}}(\omega a_T)$, where a_T denotes a shift factor which reflects the relative changes in time constants of the dynamics at each temperature. This allows one to extend the accessible frequency window up to 8−9 decades. The susceptibility peak (observed at low temperatures) is attributed to the (local) segmental relaxation governed by the dynamics of the glass transition ("glassy dynamics"). This contribution is well described by a Cole−Davidson spectral density which allows determining the segmental correlation time τ_s at the lowest temperatures; thus here τ_s is identical with a_T, and in the case of bulk PB $\tau_s = a_T$ always holds. The shift factors for other temperatures are obtained by translating the corresponding susceptibility spectra along the frequency axis to achieve a master curve. One should note that this procedure does not alter the amplitudes of the susceptibilities for individual temperatures for a given sample. Then, the slow polymer dynamics show up on the low-frequency flank of the susceptibility maximum.

Self-ordered anodic aluminum oxide (AAO) membranes with a mean pore diameter of 60 nm and a pore depth of 100 μm were prepared by two-step anodization in oxalic acid at 40 V,[23] and self-ordered AAO membranes with a mean pore diameter of 20 nm and a pore depth of 100 μm by two-step anodization in sulfuric acid at 19 V.[24] The self-ordered AAO membranes combine well-defined channel diameters with a large aspect ratio of the pores and hard-wall confinement imposed by the hydroxyl-terminated pore walls. Polybutadiene (PB) with molecular weight M = 87 kDa (polydispersity PD = 1.05), which is above $M_e \cong 2$ kDa, and with a radius of gyration $R_g \cong 11$ nm, which is well below the pore diameters of the AAO membranes, was infiltrated into the AAO.[11] The samples used here were prepared as in the case of those used in ref 11. We stress that strong efforts were undertaken to ensure that the pores of the AAO were completely filled with equilibrated PB, as controlled by weight-uptake experiments.

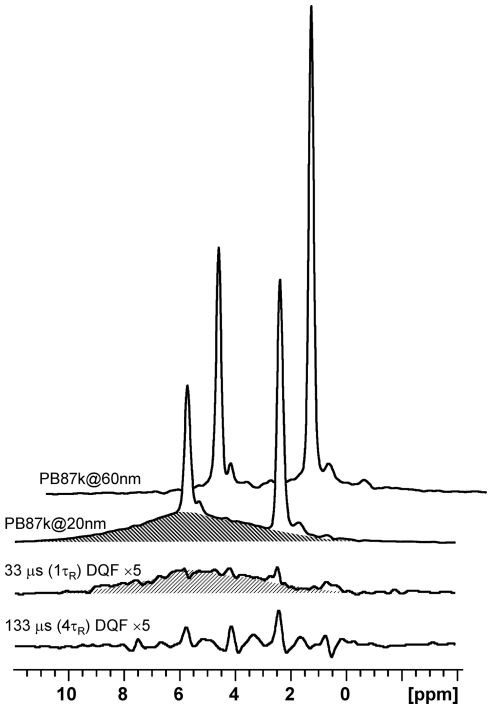

Figure 1. Fast-MAS (30 kHz) ^{1}H spectra of PB confined to AAO. The top spectrum for 60 nm membranes is shifted to the right for clarity. The background signal (shaded area) in the 20 nm spectrum corresponds to about 70% of the integral. The bottom two are double-quantum filtered spectra using the BaBa sequence[26] with the indicated recoupling times.

In order to check the quality of the samples and the origin of the ^{1}H NMR signals that are detected under low-resolution conditions, magic-angle spinning (MAS) ^{1}H NMR spectra of grinded samples were taken at 30 kHz spinning frequency in a Bruker 2.5 mm double-resonance MAS probe on a 600 MHz Avance III spectrometer equipped with a narrow-bore magnet. The spectra of the confined samples (top two traces in Figure 1) exhibit sharp PB resonances that are expected for a mobile phase. The spectra were taken under identical conditions with roughly equal sample weights; thus, the lower PB content in the 20 nm pores directly reflects the lower porosity of these AAO membranes. In the 20 nm sample, a significant broad unresolved background signal of about 70% integral further indicates substantial ^{1}H signal contributions from aluminum oxide-related −OH and H_2O species. The width and shape of this background signal are typical and have been observed before in precipitated silica samples.[25] It reflects the inhomogeneous broadening arising from a variety of different H-bonded environments. Assuming these species to consist of water with typical density, this large amount would correspond to a surface layer of about 4.5 nm thickness, which is clearly unrealistic for the 20 nm pores that do contain the polymer volume expected from the porosity of the samples. Since the 60 nm pores contain no

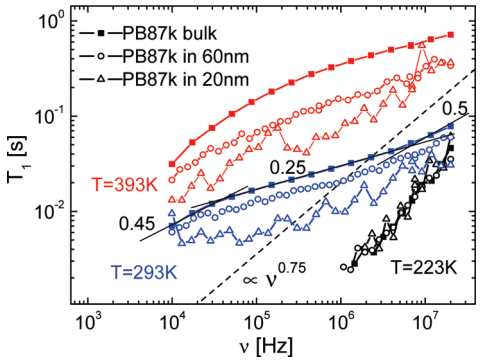

Figure 2. Spin−lattice relaxation dispersion of bulk PB $M = 87$ kDa and confined in AAO pores of 20 and 60 nm diameter at temperatures as stated. The power-law predicted by the tube-reptation model for regime II (dashed line) is included. For $T = 293$ K the power-law regimes for bulk PB according to Kimmich and Fatkullin[1] are drawn (solid lines).

significant background signal (certainly less than 10%), we attribute the difference to the different preparation (anodization) conditions of the samples and assume that most of this signal is associated with the bulk alumina phase, which thus appears hydrated to a certain degree when sulfuric acid is used as medium.

Following our previous work,[25] we have applied DQ filtering (DQF) in order to check the state of mobility of the ^{1}H species on the basis of the homonuclear dipolar coupling strength. At the shortest recoupling time, about 20% of the broad background signal is converted into DQ coherence, which is a typical value for a rigid organic solid.[25] The −OH/H_2O signal contribution must thus exhibit a static ^{1}H line width of tens of kilohertz and decays within the first ∼20 μs of a FID. In our previous static-NMR work,[11] contributions of this signal were suppressed using a mobility filter, and for the FC data reported herein, it is not expected to contribute much to the signal either, as a result of the long dead time of the instrument. At longer recoupling times, the mobile (weakly dipolar-coupled) signal contributes increasingly to the DQF signal, as expected. Unfortunately, the quality of these spectra deteriorates as a result of (correlated) noise due to the low sample amount and possible coil vibrations. Notably, at short DQF times, there are no broader resonances at the PB signal positions, indicating the virtual absence of immobilized PB in these samples, which is expected for this nonpolar polymer.

RESULTS

Figure 2 shows selected data for the dispersion of the ^{1}H spin−lattice relaxation time $T_1(\nu)$ of PB $M = 87$ kDa in the bulk melt and infiltrated in AAO membranes with pore sizes of 20 and 60 nm, each measured at 223, 293, and 393 K. One recognizes that at $T = 393$ K $T_1(\nu)$ significantly decreases with the confinement size. A somewhat smaller effect is observed at $T = 293$ K. For $T = 223$ K the relaxation dispersion virtually agree. It appears that the confinement effect becomes smaller for lower temperatures, which is in agreement with our previous DQ NMR data.[11] For bulk PB at 293 K the three power-law regimes for $T_1(\nu)$ described by Kimmich and Fatkullin[1] (and marked in Figure 2 by solid black lines) well reproduce our data. In addition, we show in Figure 2 the prediction of the tube-reptation model (regime II) which according to the corset effect is assumed to hold in confinement. Approximately such a power-law ($T_1(\nu) \propto \nu^{0.75}$) behavior is observed only at low temperatures, however, for both bulk and confined polymers. Moreover, at such low temperatures the polymer relaxation is shifted beyond the FC NMR frequency window, and the dominating local segmental relaxation leads to a strong dispersion close to $T_1 \propto \nu^1$ that is typical around $\omega\tau_s \cong 1$. This situation will become clearer when inspecting the data in the susceptibility representation (see below).

In our previous studies of bulk PB[12,13] we have shown that the relaxation changes observed while cooling originate from shifting the relaxation spectrum through the actual frequency window available for the FC NMR technique. Exploiting FTS the full relaxation spectrum can be covered and three relaxation regimes (0, I, II)[13,15] are disclosed. This is demonstrated in Figure 3a where the master curves for all three samples are shown; i.e., the susceptibility (cf. eq 2) is plotted as a function of ωa_T where a_T is the already discussed shift factor (cf. Experimental Section). Although the susceptibility master curves exhibit slightly different amplitudes, very similar relaxation dispersion is seen. This is demonstrated by multiplying the amplitude of each master curve by a factor which leads to an agreement in the low-frequency regime (Figure 3b). In the frequency range of $\omega a_T < 0.02$, in which the relaxation contributions from the collective polymer dynamics dominate, the relaxation dispersion of all three samples overlaps. This means that qualitatively the polymer specific dynamics do not change with respect to that of bulk PB. In the region $\omega a_T \cong 1$, the (local) segmental relaxation determines the relaxation, and a weak, however systematic, effect is observed: In Figure 3b, the susceptibility maximum with respect to the low-frequency part gets somewhat larger for smaller pore sizes. This may be interpreted as an indication that the spectral contribution of the segmental relaxation increases with decreasing confinement size. In other words, the fraction of polymer specific relaxation determined by the so-called order parameter[13] decreases, say, by a factor 2−3.

Figure 3 includes as line the power-law predicted by the tube-reptation model for regime II. This behavior is not observed except as the expected asymptote at the lowest frequencies and of a small region around the susceptibility maximum. The latter region corresponds to the T_1 measured at 223 K and is clearly determined by the segmental dynamics.

Upon constructing the master curves in Figure 3, the frequency shifts applied for each relaxation dispersion (measured at a given temperature) yield a shift factor a_T. Its temperature dependence is plotted in Figure 4. Clearly, the time constants diverge at high temperatures. For a smaller confinement size the shift factor becomes larger, indicating that the polymer dynamics slow down. The confinement effect, however, disappears at low temperatures where the time constants for all samples essentially agree and a_T becomes identical with τ^*. There, as mentioned before and seen in Figure 2, the relaxation data essentially coincide. In other words, when probing the glassy dynamics (at low temperatures) by FC ^{1}H NMR no change in the confinement is observed; however, when probing polymer dynamics (at high temperatures), the dynamics slow down. This is in full agreement with the NS results[7,8] mentioned in Introduction where glassy dynamics have been found unchanged while Rouse dynamics slowed down in confinement (cf. Discussion).

The susceptibility curves in Figure 3b are scaled to achieve the best agreement in the frequency range reflecting polymer dynamics ($\omega\tau_s \ll 1$). We now come back to the unscaled data in Figure 3a, for which the original T_1 data (cf. Figure 2) were just multiplied by the frequency and shifted along the frequency axis. A systematic decrease of the amplitude of the entire master curves is observed with decreasing the confinement size.

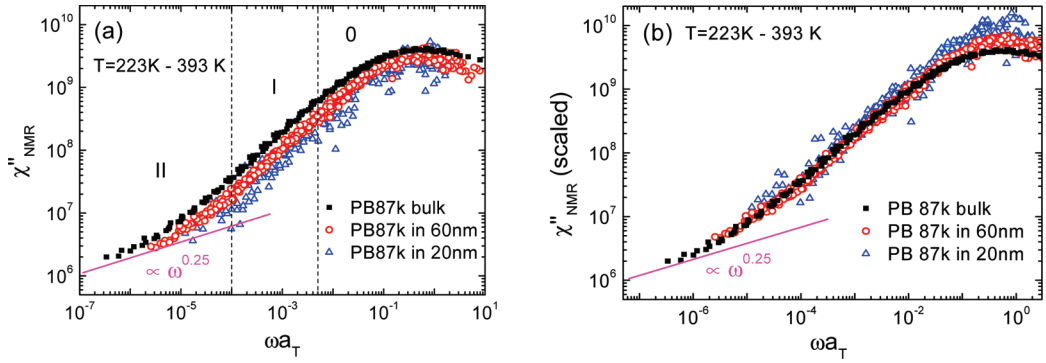

Figure 3. Susceptibility master curves of bulk PB 87 kDa and confined in 60 and 20 nm AAO obtained among others from the data in Figure 2 converted to the susceptibility representation (cf. eq 2). (a) Unscaled as-processed data; relaxation regimes (0, I, II) are indicated. (b) Scaled to agree in the low-frequency regime ($\omega\tau_s \ll 1$); the solid lines indicate the prediction for regime II of the tube-reptation model.

The area under the susceptibility is a measure of the effective coupling constant C (cf. eq 1). As discussed in the Experimental Section (cf. Figure 1), the pores of the samples contain OH groups which potentially lead to cross-relaxation with the PB protons. Assuming that this effect can be neglected and no additional relaxation contributions appear beyond those displayed in Figure 4 (e.g., some secondary (β) relaxation process could appear at very high frequencies), we can conclude that the coupling constant significantly changes in confinement. Taking the height of the susceptibility maximum as a measure of the coupling C, we find for $C/C_{bulk} = 0.61 \pm 0.05$ for 60 nm and $C/C_{bulk} = 0.34 \pm 0.1$ for 20 nm confinement. The apparent coupling constant appears to decrease by a factor of 3 for the 20 nm sample. Of course, in the case of the 20 nm sample the scatter is quite large due to the low filling factor, and the corresponding value has to be taken with care.

The coupling constant C reflects the internuclear distances r_{ij} of the spin pairs in the polymer melt, explicitly[27]

$$\int_0^\infty 1/T_1(\omega)\, d\omega = \frac{5\pi}{2} C$$
$$C = \frac{2}{5}\left(\gamma^2\hbar\frac{\mu_0}{4\pi}\right)^2 I(I+1)\sum_{i>j} r_{ij}^{-6} \quad (3)$$

where γ denotes the gyromagnetic ratio, μ_0 the magnetic constant and I the nuclear spin, the decrease of C up to a factor 3 in the confinement is a quite remarkable effect which cannot be easily explained by assuming some changes of the conformational structure of the polymer chains in the confinement. The coupling constant contains intramolecular and intermolecular contributions. Indeed, by diluting a protonated PB polymer in a deuterated PB matrix in order to suppress the intermolecular relaxation contribution, the coupling constant may change by a factor of, say, 2. Such a strong dilution in terms of a correspondingly decreasing density of the polymer melt is not expected in confinement. The density (scaling with r_{ij}^{-3}) has to change by a factor of $\sqrt{3} \cong 1.7$ to alter the intermolecular relaxation contribution by a factor 3. Another possibility is that the polymer infiltrated in the AAO membranes contains voids which would diminish intermolecular proton−proton spacing. Again, such a situation appears not plausible, especially because the polymer dynamics do not qualitatively change in confinement. Thus, at present, it is difficult to explain the change of the apparent coupling constant.

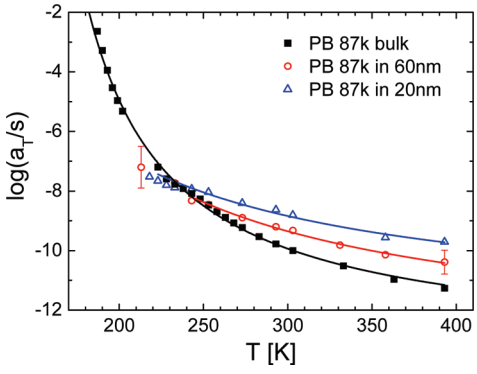

Figure 4. Temperature dependence of the shift factor characterizing the time constant of the dynamics of PB in bulk and confinement. For bulk PB the low-temperature data are from dielectric spectroscopy.[12] Lines are interpolations by the Vogel−Fulcher−Tammann law.

DISCUSSION AND CONCLUSIONS

In order to critically verify the existence of the corset effect, we have investigated the dynamics of PB in AAO confinement, a polymer-confinement system not studied before. In accordance with Kimmich, Fatkullin, and co-workers, a confinement effect is observed although the size of the confinement is larger than the polymer size in the melt; yet, the effect is less pronounced than in the case of Kimmich's data. Moreover, we do not observe the power-law relaxation typical for regime II of the tube-reptation model. Thus, the corset effect in the sense suggested by Kimmich and Fatkullin is not present for our samples. In contrast, our experimental findings demonstrate that the spectral shape of the susceptibility in the range, for which contributions from ("local") glassy dynamics dominate, is not changed. However, the time scale determining the polymer dynamics becomes longer in the confinement. A decrease of the order parameter is found; i.e., the strength of the collective polymer dynamics is reduced in confinement. As mentioned, NS experiments by Krutyeva et al.[7] and Martin et al.[8] have revealed that for PEO in AAO matrices the glassy dynamics is not changed whereas Rouse dynamics slow down in agreement with our findings. Field-cycling ^{1}H NMR essentially probes Rouse dynamics (regime I) and the onset of regime II of the tube-reptation model (cf. Figure 2a),[13,15] and these dynamics slow down in confinement. Here, a comment is worthwhile. With the NS results at hand, the change of the polymer dynamics in the confinement must not be interpreted as being a consequence of an

increase of the segment correlation time or, equivalently, monomeric friction coefficient. Such an interpretation has been done in a simulation work where again a uniform slowing down of all the modes has been observed for polymer melts in contact with nanoparticles.[28] It appears that the relationship between τ_s and Rouse time τ_R is altered in each confinement; they get more separated when the pore sizes decrease.

Investigating the changes of the dynamics for confinements of micrometer scales, i.e., under weak confinement conditions, Kimmich and co-workers[6] have reported perceptible, but small, changes with respect to the bulk behavior. As in the simulation work,[28] the authors have explained the effects by a mere change of the segmental time constant τ_s. A change by a factor of about 2 for the crossover from bulk to 800 nm confinement has been found, and they have argued that this is the first stage of the corset effect. Again, in light of the results from NS and the present FC NMR study, these findings have to be reinterpreted in such a way that only polymer dynamics slow down.

Referring to the ^{1}H spectra shown in Figure 1, a significant amount of protons from the hydroxyl groups is observed in the case of the 20 nm sample. We stress that due to the characteristics of the FC NMR experiment one only probes the relaxation of the liquid part of the NMR signal; any solid-state signal is suppressed since the free induction decay (FID) is monitored at long times where it reflects only the signal from the polymer melt. The magnetization relaxes exponentially; hence, no long-lived dynamic heterogeneities are present.

Regarding the segmental relaxation in polymer films, i.e., in 1d confinement, Serghei and Kremer[29] have claimed that no confinement effects are observed as long as the confinement size is larger than 10 nm. However, this concerns the local segmental dynamics in the microsecond−second regime as typically probed by dielectric spectroscopy. The present FC NMR results as well as those of the Kimmich group clearly demonstrate that for 2d as well as 1d confinement the polymer dynamics are affected up to confinement sizes of 1600 nm,[6] i.e., for pore sizes much larger than Flory radius of the polymer. This phenomenon is still not understood. Further experiments are needed, in particular, for samples containing larger confinement sizes in order to identify the crossover from confinement to bulk behavior for PB in AAO membranes.

AUTHOR INFORMATION

Corresponding Author

E-mail: ernst.roessler@uni-bayreuth.de.

Present Addresses

[||]Institute of Physics, Jagiellonian University, Reymonta 4, 30 059, Krakow, Poland.

ACKNOWLEDGMENT

The financial support of priority program SPP 1369 "Polymer-Solid Contacts: Interfaces and Interphases" (RO 907/16) and of the DFG grant RO 907/14 is acknowledged.

REFERENCES

(1) Kimmich, R.; N. Fatkullin, N. *Adv. Polym. Sci.* **2004**, *170*, 1–113.
(2) deGennes, P. G. *J. Chem. Phys.* **1971**, *55*, 572.
(3) Doi, M.; Edwards, S. F. *The Theory of Polymer Dynamics*; Oxford Science Publications: New York, 1986.
(4) Mattea, C.; Fatkullin, N.; Fischer, E.; Beginn, U.; Anoardo, E.; Kroutieva, M.; Kimmich, R. *Appl. Magn. Reson.* **2004**, *27*, 371.
(5) Fatkullin, N.; Kimmich, R.; Fischer, E.; Mattea, C.; Beginn, U.; Kroutieva, M. *New J. Phys.* **2004**, *6*, 46.
(6) Kausik, R.; Mattea, C.; Fatkullin, N.; Kimmich, R. *J. Chem. Phys.* **2006**, *124*, 114903.
(7) Krutyeva, M.; Martin, J.; Arbe, A.; Colmenero, J.; Mijangos, C.; Schneider, G. J.; Unruh, T.; Su, Y.; Richter, D. *J. Chem. Phys.* **2009**, *131*, 174901.
(8) Martin, J.; Krutyeva, M.; Monkenbusch, M.; Arbe, A.; Allgaier, J.; Radulescu, A.; Falus, P.; Maiz, J.; Mijangos, C.; Colmenero, J.; Richter, D. *Phys. Rev. Lett.* **2010**, *104*, 197801.
(9) Kimmich, R.; Fatkullin, N. *Macromolecules* **2010**, *43*, 9821.
(10) Kimmich, R.; Fatkullin, N. *J. Chem. Phys.* **2011**, *134*, 057101.
(11) Ok, S.; Steinhart, M.; Serbescu, A.; Franz, C.; Chavez, F. V.; Saalwächter, K. *Macromolecules* **2010**, *43*, 4429.
(12) Kariyo, S.; Brodin, A.; Gainaru, C.; Herrmann, A.; Schick, H.; Novikov, V. N.; Rössler, E. A. *Macromolecules* **2008**, *41*, 5313.
(13) Kariyo, S.; Brodin, A.; Gainaru, C.; Herrmann, A.; Hintermeyer, J.; Schick, H.; Novikov, V. N.; Rössler, E. A. *Macromolecules* **2008**, *41*, 5322.
(14) Herrmann, A.; Novikov, V. N.; Rössler, E. A. *Macromolecules* **2009**, *42*, 2063.
(15) Herrmann, A.; Kariyo, S.; Abou Elfadl, A.; Meier, R.; Gmeiner, J.; Novikov, V. N.; Rössler, E. A. *Macromolecules* **2009**, *42*, 5236.
(16) Strobl, G. *The Physics of Polymers*; Springer: Berlin, 1996.
(17) Chavez, F. V.; Saalwächter, K. *Phys. Rev. Lett.* **2010**, *104*, 198305.
(18) Chavez, F. V.; Saalwächter, K. *Macromolecules* **2011**, *44*, 1549.
(19) Vega, J. F.; Rashtogi, S.; Peters, G. W. M.; Meijer, H. E. H. *J. Rheol.* **2004**, *48*, 663.
(20) Abdel-Goad, M.; Pyckhout-Hintzen, W.; Kahle, S.; Allgaier, J.; Richter, D.; Fetters, L. J. *Macromolecules* **2004**, *37*, 8135.
(21) Abou Elfadl, A.; Kahlau, R.; Herrmann, A.; Novikov, V. N.; Rössler, E. A. *Macromolecules* **2010**, *43*, 3340.
(22) Bloembergen, N.; Purcell, E. M.; Pound, R. V. *Phys. Rev.* **1948**, *73*, 679–715.
(23) Masuda, H.; Fukuda, K. *Science* **1995**, *268*, 1466.
(24) Jessensky, O.; Müller, F.; Gösele, U. *Appl. Phys. Lett.* **1998**, *72*, 1173.
(25) Saalwächter, K.; Krause, M.; Gronski, W. *Chem. Mater.* **2004**, *16*, 4071.
(26) Feike, M.; Demco, D. E.; Graf, R.; Gottwald, J.; Hafner, S.; Spiess, H. W. *J. Magn. Reson., Ser. A* **1996**, *122*, 214.
(27) Abragam, A. *The Principles of Nuclear Magnetism*; Clarendon Press: Oxford, 1961.
(28) Dionne, P. J.; Ozisik, R.; Picu, C. R. *Macromolecules* **2005**, *38*, 9351.
(29) Serghei, A.; Kremer, F. *Macromol. Chem. Phys.* **2008**, *209*, 810.